INTERNAL STRAIN MEASUREMENT AND IMPACT RESPONSE OF 3D WOVEN CARBON FIBRE COMPOSITES

J. Broderick[1], E. Archer*[1], A. McMillan[2], AT. McIlhagger[1]

[1]*Engineering Composites Research Centre, University of Ulster, Jordanstown, Northern Ireland, BT37 0QB.*
[2]*Faculty of Advanced Technology, University of Glamorgan, Pontypridd, CF37 1DL*
Corresponding author (e.archer@ulster.ac.uk)

Keywords:
3D woven composite, Fibre optic sensors

Abstract
Extrinsic Fabry Perot Interferometer (EFPI) fibre optic sensors have been utilised to measure the internal matrix strain in a three dimensionally woven carbon fibre reinforced polymer composite. EFPI sensors were embedded at two levels within a four layer 3D woven composite, and comparison surface measurements were provided through resistive strain gauging and biaxial extensometry. A variation in tensile modulus of as much as 24% was found from internal measurement compared with the material surface. Through correlation with micro-graphical analysis, a link between the variations in mechanical performance and localised variations in fibre volume fraction could be established. Furthermore, the impact performance was measured.

1. Introduction

3D woven textile reinforced composites allow the optimisation and tailoring of specific material properties into the final component that can provide a reduction in manufacturing cost, have higher ballistic damage resistance and impact tolerance than 2D materials, higher tensile strain and strain-to-failure values, and also higher interlaminar fracture toughness [1]. However, earlier research [2] showed that where the binder travels through the thickness of the fabric a resin rich area is created. This work will measure the strain (under tensile loading) at different levels from within this region i.e. a method of strain sensing will be used to measure the strain within the resin pockets created by the binder at different levels within the 3D composite structure. This will provide data that should measure the effect of the hypothesised changes in fibre volume fraction caused by the binder. It will also provide data for direct correlation with subsequent works endeavouring to model this type of material. Extrinsic Fabry Perot Interferometer (EFPI) sensors were embedded at two levels within a four layer 3D woven composite and comparative surface measurements were provided through resistive strain gauging and biaxial extensometry. A fibre optic sensing system was selected as it has been shown that they can be successfully embedded within the carbon fibre reinforced composite (CFRP) structure without causing degradation in the performance of the material [3, 4]. They have been successfully employed in this strain sensing role within CFRP materials in several studies to measure fatigue strains [5], impact damage [6, 7] delamination [8], flexural strains [9] and tensile strains [10]. Oliveira et al [11] outline that EFPI sensors offer a greater level of sensitivity to strain measurement when compared to other fibre optic

strain sensing systems such as Bragg grating sensors. Leng [12] and Liu [13] both outline that EFPI strain sensors are insensitive to temperature change. Leng goes further to explain that this is due to the coefficients of thermal expansion of the quartz capillary tube and the optical fibre, used in the construction of the EFPI sensor, are nearly identical and therefore the sensor will not pick up thermally induced strains as both constituent materials will expand and contract at the same rate. Through correlation with micro-graphical analysis, a link between the variations in mechanical performance and localised variations in fibre volume fraction could be established. The 3D multi-layer reinforcements were manufactured on a textile loom with mechanical modifications to produce preforms with fibres orientated in the warp, weft and through-the-thickness (TTT) directions. Angle Interlock 3D woven composites have previously been shown to provide manufacturing advantages, yet also provide a structure where the advantages of low crimp tows bound together by a binder tow, result in a composite with high performance and reduced sensitivity to interlaminar shear [14].

2. Experimental

3D multi-layer woven reinforcements were designed using the X-Sectional design system to provide a representation of the structure, detailing the relative positions of the yarns and also generating the lifting plan to operate a Jacquard controlled loom. Fabrics were then manufactured on a conventional textile loom with mechanical modifications. The loom used was a DATAWEAVE powerloom with a flexible rapier and Jacquard controller incorporating 1152 hooks. The 3D woven carbon fibre fabric reinforcement was produced with an angle interlock binding arrangement with yarn parameters of; Toho Tenax HTS 2x12K Warp, Toho Tenax HTS 12K Weft, Toho Tenax HTA 6K binder (Table 1&2). The produced fabric (Fig. 1) had an areal density of 2640gsm and 16 picks/cm with a 6% binder content. This fabric style/design was selected as the minimal binder content would maximise in-plane performance whilst retaining the improved through the thickness properties provided by having a binder. There are also sources of published mechanical performance data available which can be directly compared to the data collected through this investigation [2, 14].

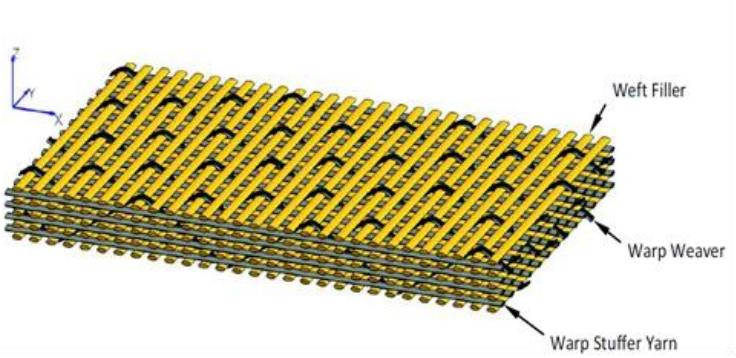

Figure 1. Angle Interlock Woven Structure.

Table 1. Details of fabric.

	Warp	Weft	Binder content (%)	Binder type	Areal weight (g/m²)
Angle interlock	2 x12k HTS	12k HTS	6	6k HTA	2720

Table 2. Details of fibres used.

	Tensile strength (MPa)	Tensile modulus (GPa)
HTA	**3950**	**238**
HTS	**4300**	**240**

A novel method of sensor integration was developed whereby thin walled PTFE tubing, of dimension 1.02mm outside diameter and 0.2mm wall thickness, was woven into the fabric along with selected warp yarns. Once off the loom, the preform was cut into the required dimensions and placed within the processing tooling, the sensors were threaded through the PTFE tubing to their pre-determined location within the fabric. In this case the location chosen for interrogation was the resin rich pockets created by the binder. The distance from the selected binder, visible on the surface of the fabric, to the edge of the preform was measured. The sensor head was then threaded through the PTFE tubing for this exact distance. This ensured that the sensor head would be embedded in the resin pocket created by the binder. The sensor was then secured from movement with flash tape and the PTFE tubing was drawn out of the fabric leaving the sensor in the desired location. EFPI sensors were embedded between layer 1 and 2, and layers 3 and 4 of the 4 warp layer fabric. This arrangement was selected as these positions would be expected to have a significant difference in Vf (depicted in Figure 2) and therefore tensile performance. The EFPI sensors were integrated in such a fashion to produce the final test coupons with one embedded EFPI sensor located along the central axis in the warp, loading direction beside the targeted binder at the chosen depth/layer within the fabric. Fabrics with embedded EFPI sensors were infused with polymer and processed into composites via a modified VaRTM technique. The modified VaRTM tooling included a layered arrangement of 2 silicon rubber sealing gaskets to allow for the sensor optical fibres to pass through the tooling cavity wall without the reduction in vacuum integrity. Additional clamping bolts were utilised to ensure no loss of vacuum. To ensure sensor survival during the moulding process and handling post manufacture, the portions of optical fibre lead that exited the material were protected with a piece of thin walled silicon rubber tubing of internal diameter 1mm and a wall thickness of 1mm. The operation of an EFPI sensor is based on the multi-reflection Fabry-Perot interference between two reflected mirrors where ‘s’ is the cavity length (distance between two mirrors) and L is the gauge length. The basic sensing principle is that the cavity length ‘s’ changes with the application of mechanical strains. ‘s’ is measured from the modulation in the reflection spectrum by counting the number of fringes over a specified wavelength range.

$$s = \frac{m\lambda_1\lambda_2}{2(\lambda_2 - \lambda_1)} \tag{1}$$

Where the phase difference between λ_1 and λ_2 is $2m\pi$ and m is an integer.

The change in ‘s’ can be expressed as:

$$\Delta s = L\varepsilon + A\Delta T \tag{2}$$

Where

ε = strain on sensor

L = gauge length

ΔT = change in environment temperature

A = change in sensor length due to temperature = $L(\alpha_q - \alpha_f)$

Where α_q and α_f are the thermal coefficient of expansion for the polyimide-coated hollow core fibre (quartz capillary) and the single mode optical fibre respectively.

Hence, strain on the sensor is calculated [15]:

$$\varepsilon = \frac{\Delta s}{L} \tag{3}$$

The EFPI strain sensing system used in this investigation was an "off the shelf" commercially available system sourced from Luna Innovations. The system was a FibrePro2 System which, when coupled with a MUX8 Channel Expansion Module, could monitor and record the response from 8 individual EFPI sensors, simultaneously. The particular sensors used for this investigation were supplied by Luna Innovations and had part number: ES-RM-01M-BP. These sensors had a 10mm gauge length with a 1m optical fibre lead and FC connectors rated up to 200°C. These sensors had a resolution of 1με or 1nm and were supplied with a polyimide coating specifically engineered for use with epoxy matrix composites.

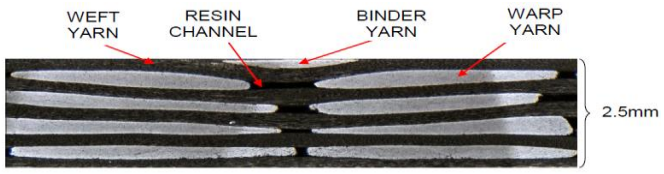

Fig 2. Micrograph taken in the warp direction showing the changing resin rich regions caused by the binder displacing warp yarns in an angle-interlock 3DWCFRP.

Fabrics were infused with the 2 part epoxy resin system of Araldite® LY-564 resin and Aradur® HY-2954 hardener, manufactured by Hunstman. This system is mixed to the ratio of 100g of resin to 35g of hardener as per the manufacturer's instruction. Prior to processing the resin was degassed for 1 hour at 30˚C after mixing to the two constituents. Once the tooling temperature has equilibrated at 75°C, resin was injected in to the tool cavity until the fabric has been completely infused. The tooling temperature was then ramped to 100°C and held isothermal for 1 hour. The composite was then de-moulded and post cured at 145°C for 4 hours to achieve a Tg of 140°C. Fibre volume fraction was measured/calculated via the density buoyancy method. The processed 3D woven carbon fibre reinforced plastic (3DWCFRP) for this investigation had a Vf 58.67% +/- 1.3% which is comparable to similar materials produced through works by Archer [2] and Buchanan [14]. Test coupons were cut from the moulded composite plates via high pressure water jet cutting on an OMAX 2626 Jet Machining Centre. Tensile tests were carried out in accordance with BS EN ISO 527-4:1997 on a Zwick Z100 Universal testing machine. To allow for adequate correlation and reliability in fibre optic strain measurement, test coupons with an embedded EFPI sensor were further instrumented with a restive strain gauge bonded to their surface adjacent to the location of the EFPI sensor. The restive strain gauges were sourced from Vishay Precision Group and were of model range 500UW and had a gauge length of 12.7mm, grid resistance of 350Ω and a gauge factor of 1.2. This model of gauge was selected for its similar gauge length to that of the EFPI fibre optic gauge and also its compatibility to mounting to the epoxy matrix surface. Further strain measurement was taken through a biaxial extensometer directly linked to the Zwick Z100 Universal testing machine. Samples were tested up to a maximum load of 3kN with simultaneous strain measurement taken from the embedded EFPI sensor, resistive strain gauge and the biaxial extensometer. Force was recorded through the load cell of the testing

machine. Samples tested were all taken from one preform/composite plate of which one half contained EFPI sensors embedded between warp layers 1+2, and the other half containing EFPI sensors embedded between warp layers 3+4. The preform/composite was woven/produced in such a way that each coupon would have 1 EFPI sensor embedded along the central axis, running in the warp direction of the weave pattern but located either between layers 1+2 or between layers 3+4.

Further specimens were impacted according to ASTM D7136/D163M -05 using an Instron 9200 Series drop weight impact tester. Low velocity impact loads were imparted on the composite specimens using an instrumented drop-weight impact testing machine. Specimens were subjected to four energy levels at 10, 20, 30 and 40 joules by keeping the mass constant (13.91 kg) and varying the drop height. Computed tomography (CT) was then used to observed damage using a Phoenix v|tome|x s from GE equipped with a Perkin Elmer flat panel (512x512 px, 400 µm pix size). The X-ray tube was operated at 150 kV and 230 µA. The Voxel resolution was 41 µm.

3. Results

Presented below, Figures 3 & 4, are stress/strain responses measured by the respective techniques during the tensile testing of a coupon in which the EFPI sensor was embedded in the resin channel between layers 1+2, and also a coupon where the EFPI sensor was embedded in the resin channel between layers 3+4. The tensile modulus was used as means of comparison of the change in mechanical performance at the different positions within the composite. Figure 3 illustrates that the strain measurement from between layers 1+2 is in close agreement with the strain measurements taken on the surface of the material by the conventional techniques. Conversely Figure 4 shows the strain measurement taken by an EFPI sensor embedded between layers 3+4 to be significantly lower thereby yielding a much higher tensile modulus at this point within the material. Once again the conventional surface measurements are in close agreement. Two observations noted here are that the EFPI sensors have returned a measurement of similar accuracy to that of the resistive strain gauges and the biaxial extensometer, and also that the signal noise picked up the extensometer measurement was due to the small strains being experienced/measured due to the high stiffness of this composite. Table 3 represents a summary of the data measured by each technique from the test program. As shown the surface measurements of tensile modulus are in close agreement with the EFPI measurement taken from between layer 1+2 but there is a significant increase in tensile modulus between layers 3+4. This is highlighted by the tensile modulus measured between layer 1+2 being 1.9% larger than the surface measured modulus and then additionally the modulus measured between layers 3+4 is 24% greater than that at the surface. The surface modulus measurements being in close agreement with those presented by Archer [2] and Buchanan [14] for a similar material. The measurement of varying tensile modulus at differing positions within the 3DWCFRP structure demonstrates the anisotropic mechanical nature of the material. Bogdanovich [16] presented data in which internal flexural modulus measurements taken by an embedded EFPI sensor within a 3DWCFRPC were higher than that measured by surface mounted strain gauges. It was hypothesized by this work that this was due to the EFPI sensor being embedded within a region of higher fibre volume fraction, however no evidence of this was presented. This current investigation has gone further in showing that not only can there be a difference between in strain induced on the surface and the strain induced internally within the 3DWCFRPC. But there can also be differences in the strain measured at varying locations within a 3DWCFRPC. To explain the strain distribution recorded by this investigation and to investigate any relationship with changes in fibre volume

fraction, it was necessary to dissect a sample of the tested coupons and examine the structure of the tested materials through micro-graphical analysis. Figures 5 and 6 are a result of this analysis. Figure 5 shows that the EFPI sensor between layers 1 and 2 is embedded within the resin channel at this level and is in an area of localised low fibre volume fraction. Whereas, conversely, Figure 6 shows that the EFPI sensor between layers 3 and 4 has been embedded in the resin channel but it is surrounded by both its adjacent warp tow and the binder and is therefore in an area of localised high fibre volume fraction. This links the changing tensile modulus to visible variations in fibre volume fraction as the regions in which high values of tensile modulus were measured, between layers 3&4, are the regions in which it can be seen to have an increase in fibre volume fraction.

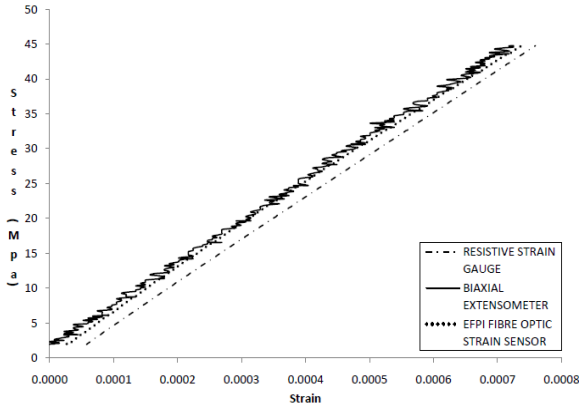

Fig.3. Graph of Stress Vs Strain from the tensile test of a coupon with an EFPI sensor embedded between layers 1+2.

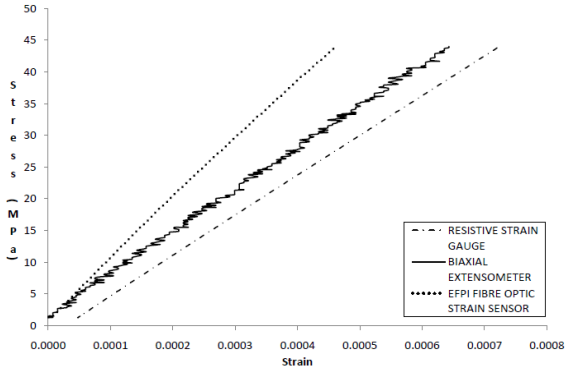

Fig.4. Graph of Stress Vs Strain from the tensile test of a coupon with an EFPI sensor embedded between layers 3+4.

Table 3. Comparison of tensile modulus measurements taken by each measurement technique from each of the tested samples.

	RESISTIVE STRAIN GUAGE	BIAXIAL EXTENSOMETER	EFPI FIBRE OPTIC SENSOR EMBEDDED BETWEEN LAYER 1+2	EFPI FIBRE OPTIC SENSOR EMBEDDED BETWEEN LAYER 3+4
MEAN	60.69 GPa	60.19 GPa	61.67 GPa	80.18 GPa
STANDARD DEVIATION	3.09	2.79	6.09	10.95
COEFFIECIENT OF VARATION	5.09	4.65	9.88	13.67

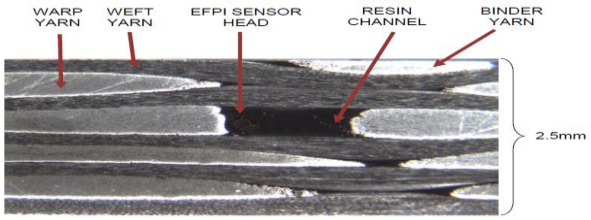

Figure 5. Micrograph taken in the weft direction showing EFPI sensor embedded in the resin channel in warp layer 2.

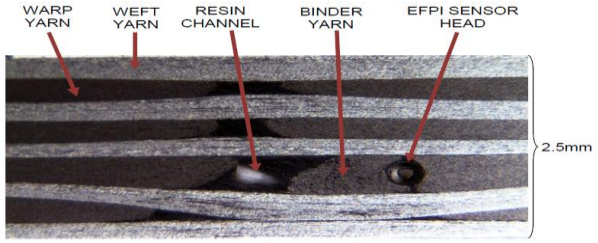

Fig 6. Micrograph taken in the weft direction showing EFPI sensor embedded in the resin channel in warp layer 3.

Table 4 gives the results of dynamic impact response of the laminates for the four energies tested in this study. In this table are given maximum load, energy at maximum load and the total energy absorbed in the form of elastic deformation and creation of new surfaces in the form of different damage mechanisms like matrix cracking, delamination. The difference in the energy at maximum load and the total energy gives the energy that goes in creating the new surfaces. The plot of entire dynamic history in terms of load versus displacement gives qualitative information on the state of damage in the laminate. Figure 7 shows the load displacement response at the 4 energies. It can be seen from these plots that the general response of the three types of laminate is the same. As the impact energy increases, there is increase in the peak load, energy to maximum load, slope of the load-time curve, and the total energy. However, it was found that the time to peak load and total duration of impact reduces with the increase in the impact energy.

Table 4. Impact test results.

Impact Energy J	Max load kN	Energy at max laod J	Total Energy J
10	4.01	9.92	3.43
20	4.90	16.11	12.03
30	4.89	14.81	30.70
40	4.84	15.30	31.23

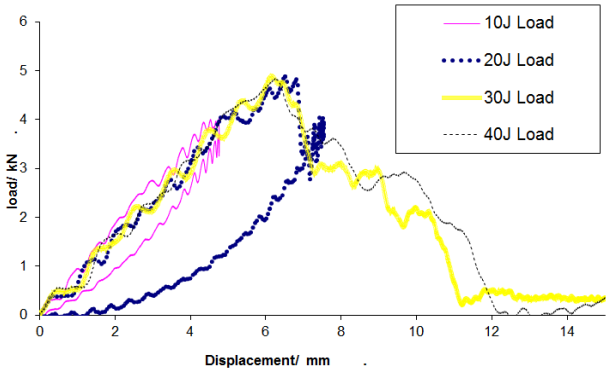

Fig 7. Impact load Vs displacement for 4 energy values.

4. Conclusion

The goal of this investigation was to accurately control the placement of a sensory system that could investigate the anisotropic nature of a 3DWCFRPC. This was achieved and it was possible to attribute changes in tensile modulus with changes in fibre volume fraction at different positions within the composite structure showing agreement with original hypotheses that "resin rich regions" or resin channels are regions of high strain.

5. Acknowledgments

This work as funded through Rolls-Royce CAST award and Department for Employment and Learning (Northern Ireland).

References

[1] King RS., Stewart G., McIlhagger AT., Quinn JP., 'The influence of through the thickness binder yarn count on fibre volume fraction, crimp and damage tolerance within 3D woven carbon fibre composites,' Polymers and Polymer Composites, 17(5), 303 (2009).
[2] Archer, E., Buchanan, S., McIlhagger, AT., Quinn. JP., Morgan, M., 'An investigation on the effect of 3D weaving on carbon fibre tows, fabrics and composites,' Proceedings of the 9th International Conference on Textile Composites (Texcomp9), 371 (2008).
[3] J. S. Leng, A. Asundi. Real-time cure monitoring of smart composite materials using extrinsic fabry-perot interferometer and fibre bragg grating sensors. Smart Materials and Structures 11, 249-255 (2002).
[4] H. Ling. "Viability of using an embedded FBG sensor in a composite structure for dynamic strain sensing." Measurement 39, 328 – 334, (2006).
[5] V. Zetterlind. "Fatigue Testing of a Composite Propeller Blade Using Fiber-Optic Strain Sensors." IEEE Sensors Journal, Vol. 3, No. 4, 393 – 399, (2003).
[6] H. Tsuda. "Strain and damage monitoring of CFRP in impact loading using a fibre bragg grating sensor system." Composites Science and Technology 67, 1353 – 1361, (2007).
[7] A. Chambers. "Evaluating impact damage in CFRP using fibre optic sensors." Composites Science and Technology 67, 1235 – 1242, (2007).
[8] H. Ling. "Determination of dynamic strain profile and delamination detection of composite structures using embedded multiplexed fibre-optic sensors." Composite Structures 66, 317 – 326, (2004).
[9] F. Bosia. "Deformation characteristics of composite laminates – part 1: speckle interferometry and embedded Bragg grating sensor measurements." Composites Science and Technology 62, 41 – 54, (2002).
[10] T. Liu. "Simultaneous strain and temperature measurements in composites using extrinsic Fabry-Perot interferometric and intrinsic rare-earth doped fiber sensors." Sensors and Actuators A 80, 208 – 215, (2000).
[11] R. de Oliveira. "Health monitoring of composite structures by embedded FBG and interferometric Fabry-Perot sensors." Computers and Structures 86, 340 – 346, (2008).
[12] J. S. Leng, A. Asundi. Real-time cure monitoring of smart composite materials using extrinsic fabry-perot interferometer and fiber bragg grating sensors. Smart Materials and Structures 11, 249-255 (2002).
[13] T. Liu. "Simultaneous strain and temperature measurements in composites using extrinsic Fabry-Perot interferometric and intrinsic rare-earth doped fiber sensors." Sensors and Actuators A 80, 208 – 215, (2000).
[14] Buchanan, S., Grigorash, A., Archer, E., McIlhagger, AT., Quinn, JP., Stewart, G., 'Analytical Elastic Stiffness Model for 3D Woven Orthogonal Interlock Composites,' Composite Science and Technology, 70(11), 1597 (2010).
[15] J. Leng. "Structural health monitoring of smart composite materials by using EFPI and FBG sensors." Sensors and Actuators A 103, 330 – 340, (2003).
[16] A. Bogdanovich. "Fabrication of 3-D woven prefroms and composites with integrated fiber optic sensors." SAMPE, Vol. 39, 4, 6 – 15, (2003).